Supporting Information

Atomic-Scale Insights into Mechanical Properties of Calcium Silicate Hydrates: Role of Hydrogen Bond Networks and Bond Order Distributions

Neng Li[1,*], Deyong Zhou[1], Jieshuo Wan[1], Zhongyong Zhang[1], Fujie Jia[3], Jiayuan Ye[3], Xiao Zhi[2], Wei Chen[1]

[1]*State Key Laboratory of Silicate Materials for Architectures, Wuhan University of Technology, Wuhan 430070, China*

[2]*China National Building Material Group Co., Ltd, Beijing 100036, China*

[3]*State Key Laboratory of Green Building Materials, China Building Materials Academy, Beijing 100024, China*

[*]Corresponding author, E-mail: lineng@whut.edu.cn

The matrix form of the anisotropic elasticity equation is derived from the generalised Hooke's law. The elastic constants C_{ij} *and* the compliance tensor S_{ij} constituents of various calcium silicate hydrate crystalline phases were calculated using VASP based on the stress-strain response[1]. These data can be used to determine the materials' mechanical properties, including the crystalline bulk modulus (B) and shear modulus (G), which can be estimated through orientational averaging using the Voigt-Reuss-Hill method[2]. The calculation formulas for various mechanical properties are as follows:

$$B_v = \frac{1}{9}\left[C_{11} + C_{22} + C_{33} + 2(C_{12} + C_{13} + C_{23})\right] \quad (1)$$

$$B_R = \frac{1}{S_{11} + S_{22} + S_{33}} + 2(S_{12} + S_{13} + S_{23}) \quad (2)$$

$$G_v = \frac{1}{15}\left[(C_{11} + C_{22} + C_{33}) - (C_{12} + C_{13} + C_{23}) + 3(C_{44} + C_{55} + C_{66})\right] \quad (3)$$

$$\frac{15}{G_R} = 4(S_{11} + S_{22} + S_{33}) - 4(S_{12} + S_{23} + S_{13}) + 3(S_{44} + S_{55} + S_{66}) \quad (4)$$

$$B = \frac{B_V + B_R}{2} \quad (5)$$

$$G = \frac{G_V + G_R}{2} \quad (6)$$

$$E = \frac{9B}{3B + G} \tag{7}$$

$$\nu = \frac{3B - 2G}{2(3B + G)} \tag{8}$$

Table S1. CSH phase types and cell parameters used for calculations.

Lable	Phase	a (Å)	b (Å)	c (Å)	a (°)	β(°)	γ(°)	Bravais Lattice	Space Group	atom number	Dc(g/cm^3)	V(Å^3)	morphology	Ref.
a.1	clinotobermorite-2M	11.276	7.343	22.642	90.000	97.280	90.000	mC	Cc	86	2.611	955.913	layer	[3]
a.2	clinotobermorite-1A	11.274	7.344	11.468	99.180	97.190	90.030	aP	P1	86	2.611	941.4952	layer	[4]
a.3	riversideite	11.156	7.303	9.566	101.080	92.830	89.980	aP	P -1	62	2.865	788.4457	layer	[3]
a.4	kenotobermorite-4O	11.265	7.386	44.970	90.000	90.000	90.000	oF	Fdd2	88	2.460	959.907	layer	[5]
a.5	kenotobermorite-2M	6.735	7.385	22.487	90.000	90.000	123.250	mC	Cm	44	2.460	972.0657	layer	[4]
a.6	tobermorite-2M	6.732	7.369	22.680	90.000	90.000	123.180	aP	P1	87	2.278	968.3755	layer	[5]
a.7	plombièrite-2M	6.735	7.425	27.987	90.000	90.000	123.250	aP	B11b	104	2.228	1193.4229	layer	[4,6]
a.8	jennite	10.576	7.265	10.931	101.300	96.980	109.650	aP	P-1	69	2.325	746.6567	layer	[7]
b.1	foshagite	10.320	7.360	7.040	90.000	106.400	90.000	aP	P-1	40	2.736	504.5876	layer	[8]
b.2	nekoite	7.588	9.793	7.339	111.770	103.500	86.530	aP	P1	45	2.217	478.0143	non-layer	[9]
b.3	xonotlite	17.032	7.363	7.012	90.000	90.360	90.000	aP	P-1	33	2.700	455.4716	layer	[10]
b.4	calcium chondrodite	8.921	11.448	5.076	90.000	90.000	108.320	mP	P2_1/c	38	2.825	503.225	non-layer	[11]
b.5	afwillite	16.278	5.632	13.236	90.000	134.900	90.000	mC	Cc	42	2.646	877.2983	non-layer	[12]
b.6	α-C_2SH	9.487	9.179	10.666	90.000	90.000	90.000	oP	Pbca	80	2.721	951.6738	non-layer	[13,14]
b.7	dellaite	6.825	6.931	12.907	90.680	97.570	98.180	aP	P-1	48	2.966	613.8669	non-layer	[15]
b.8	jaffeite	10.035	10.035	7.499	90.000	90.000	120.000	hP	P 3	54	2.593	666.9473	non-layer	[16]
b.9	rosenhahnite	6.955	9.484	6.812	108.640	94.840	95.890	aP	P-1	36	2.897	433.7734	non-layer	[17]
b.10	suolunite	19.776	5.990	11.119	90.000	90.000	90.000	oF	Fdd2	128	2.707	1357.6065	non-layer	[18]
b.11	trabzonite	20.581	10.324	9.100	90.000	90.000	90.000	oA	Ama2	80	2.902	996.4519	non-layer	[19]
b.12	hydroxyledgrewite	15.400	5.069	11.358	90.000	100.598	90.000	mP	P2_1/c	66	2.908	881.2387	non-layer	[20]
b.13	chegemite	11.396	23.557	5.070	90.000	90.000	90.000	oP	pnma	104	2.822	1390.3494	non-layer	[21]
c.1	wollastonite	7.926	7.320	7.065	90.055	95.217	103.430	aP	P-1	30	2.916	409.9165	non-layer	[22]
c.2	kilchoanite	11.420	5.090	21.950	90.000	90.000	90.000	oI	Ima2	96	3.003	1318.6395	non-layer	[23]
c.3	katoite hydrogarnet	12.270	12.270	12.270	90.000	90.000	90.000	cI	Ia-3d	116	2.530	1027.508	non-layer	[24]
d.1	tilleyite	15.108	10.241	7.579	90.000	105.170	90.000	mP	P2_1/c	88	2.867	1166.1443	non-layer	[25]
d.2	fukalite	3.786	10.916	23.379	90.000	90.000	90.000	mP	P2_1/c	160	2.867	1984.757	non-layer	[26]
d.3	scawtite	11.039	15.194	6.634	90.000	115.645	90.000	mC	C 1 m 1	82	2.758	1021.5042	non-layer	[27]
d.4	spurrite	14.156	6.712	10.484	90.000	101.270	90.000	mP	P2_1/c	76	3.023	1004.6924	non-layer	[28]
d.5	galuskinite	18.787	6.724	10.467	90.000	90.788	90.000	mP	P2_1/c	104	3.098	1359.8678	non-layer	[29]
e.1	pectolite	7.980	7.023	7.018	90.540	95.140	102.550	aP	P-1	32	2.888	395.4902	layer	[30]
e.2	oyelite	11.250	7.250	20.460	90.000	90.000	90.000	aP	P-1	82	2.565	872.1369	layer	[31]
e.3	cuspidine	7.518	10.521	10.906	90.000	70.700	90.000	aP	P1	62	2.982	841.1488	non-layer	[32]
e.4	rustumite	7.620	18.550	15.510	90.000	104.330	90.000	mC	C2/c	156	2.921	2206.72	non-layer	[33]

Table S2. CSH phase types and cell parameters after calculations.

Label	Phase	a (Å)	b (Å)	c (Å)	a (°)	β(°)	γ(°)	V(Å3)	ΔV(%)
a.1	clinotobermorite-2M	11.41	7.46	22.70	90.00	98.25	90.00	1911.83	2.81
a.2	clinotobermorite-1A	11.44	7.45	11.60	99.85	98.31	89.71	941.50	3.64
a.3	riversideite	11.21	7.38	9.68	99.55	92.74	89.97	788.45	3.21
a.4	kenotobermorite-4O	7.50	44.99	11.21	90.00	90.00	90.00	959.91	1.08
a.5	kenotobermorite-2M	6.85	7.50	22.57	90.00	90.00	123.08	972.07	3.92
a.6	tobermorite-2M	6.80	6.87	22.63	88.45	88.71	113.39	968.38	2.99
a.7	plombièrite-2M	6.70	7.42	28.55	90.40	92.22	122.69	1193.42	1.97
a.8	jennite	10.58	7.25	10.76	100.95	97.98	109.23	746.66	-1.69
b.1	foshagite	10.27	7.31	7.02	89.97	107.04	89.96	504.59	-1.64
b.2	nekoite	7.55	9.63	7.29	111.23	104.32	87.65	478.01	-2.51
b.3	xonotlite	8.66	7.35	13.89	90.03	90.15	102.28	455.47	-1.54
b.4	calcium chondrodite	8.91	5.12	11.64	90.00	108.68	90.00	503.23	2.26
b.5	afwillite	16.36	5.68	13.39	90.00	135.16	90.00	877.30	2.06
b.6	α-C2SH	9.54	9.25	10.78	90.00	90.00	90.00	951.67	2.46
b.7	dellaite	6.89	7.00	12.97	90.95	97.57	98.19	613.87	2.52
b.8	jaffeite	10.10	10.10	7.55	90.00	90.00	120.00	666.95	1.98
b.9	rosenhahnite	7.05	9.56	6.89	108.77	95.50	95.46	433.77	3.23
b.10	suolunite	19.96	6.04	11.25	90.00	90.00	90.00	1357.61	3.08
b.11	trabzonite	20.73	6.96	6.96	97.41	90.00	90.00	996.45	3.01
b.12	hydroxyledgrewite	15.38	5.12	11.36	90.00	100.05	90.00	881.24	1.12
b.13	chegemite	11.45	23.71	5.12	90.00	90.00	90.00	1390.35	2.16
c.1	wollastonite	8.02	7.39	7.15	90.07	95.48	103.43	409.92	3.26
c.2	kilchoanite	11.55	5.14	22.23	90.00	90.00	90.00	1318.64	3.35
c.3	katoite hydrogarnet	11.01	11.01	11.01	109.47	109.47	109.47	1027.51	3.47
d.1	tilleyite	15.27	10.37	7.63	90.00	105.16	90.00	1166.14	3.03
d.2	fukalite	7.63	23.60	11.66	90.00	109.07	90.00	1984.76	2.86
d.3	scawtite	10.99	15.36	6.70	90.00	115.38	90.00	1021.50	1.82
d.4	spurrite	14.30	6.78	10.58	90.00	101.46	90.00	1004.69	2.84
d.5	galuskinite	18.98	6.79	10.56	90.00	90.91	90.00	1359.87	2.85
e.1	pectolite	8.07	7.09	7.11	90.60	95.19	102.41	395.49	3.48
e.2	oyelite	7.39	11.05	11.20	90.08	89.56	72.49	872.14	4.66
e.3	cuspidine	7.56	10.59	11.09	90.00	108.75	90.00	841.15	3.31
e.4	rustumite	7.61	18.52	15.52	90.00	104.25	90.00	2206.72	-0.27

Table S3. Major Elastic Constants (GPa) of 33 Crystal Phases.

Lable	C11	C22	C33	C44	C55	C66	C12	C23	C13
a.1	128.209	161.173	144.716	45.623	14.783	37.435	47.119	57.746	29.874
a.2	113.747	158.198	143.563	42.894	15.478	31.676	51.186	57.716	33.551
a.3	218.668	203.1656	132.5157	45.0697	44.2905	74.8718	83.266	46.504	53.499
a.4	211.391	183.302	163.892	47.23	56.731	57.515	61.869	39.12	53.551
a.5	110.297	143.6598	129.7906	33.6313	42.2163	18.3989	35.068	46.276	47.66
a.6	110.214	121.595	112.0625	31.1578	18.9985	47.8877	41.832	36.622	24.269
a.7	86.164	101.594	71.467	14.967	17.752	38.22	33.777	23.802	21.153
a.8	133.221	122.352	78.975	30.308	27.618	36.519	41.625	41.895	36.969
b.1	121.3702	176.2864	92.5794	51.98	24.5104	41.1759	37.825	46.315	19.305
b.2	85.104	110.338	115.88	30.525	24.54	24.648	40.587	35.528	49.817
b.3	139.567	172.363	106.723	51.728	35.86	48.661	43.72	40.787	29.29
b.4	177.6144	192.4353	165.294	69.4003	56.0708	66.4806	68.28	76.95	77.648
b.5	127.9913	133.9738	140.7009	27.6305	25.4731	37.1153	43.417	49.448	53.59
b.6	166.8503	158.4421	173.8462	59.4316	54.0381	51.3605	65.013	64.717	66.524
b.7	154.2956	143.4134	156.8645	38.9597	46.7335	39.0234	43.892	53.535	58.236
b.8	121.063	121.063	133.359	30.272	30.272	37.683	45.697	39.176	39.176
b.9	132.5991	170.504	141.6011	55.4421	31.3816	31.4315	40.257	56.45	29.225
b.10	95.255	126.105	119.123	43.053	41.46	43.411	26.177	52.462	32.056
b.11	217.2547	185.3913	177.86	71.1516	52.2441	53.4035	62.452	73.309	52.08
b.12	152.036	170.478	123.536	55.585	43.487	55.065	67.106	65.876	70.414
b.13	145.107	133.422	154.236	46.337	49.772	38.295	65.856	65.656	60.415
c.1	130.2675	186.6214	136.894	32.7427	32.3388	52.5864	56.911	45.197	40.419
c.2	175.4751	203.1856	187.1862	64.7637	60.324	68.0007	68.434	69.257	68.884
c.3	97.6444	97.6444	97.6444	31.4388	31.4388	31.4388	39.717	39.717	39.717
d.1	99.021	136.555	132.105	41.537	51.343	38.953	33.468	46.328	49.609
d.2	186.2294	218.214	204.7764	54.4717	47.3311	56.0888	61.025	65.834	63.228
d.3	134.596	126.868	144.563	34.347	49.398	33.986	55.248	28.516	60.952
d.4	124.205	87.931	147.124	46.543	38.257	31.168	0.047	24.811	48.808
d.5	158.899	152.734	123.657	51.828	36.169	35.479	43.818	44.905	54.009
e.1	151.189	212.208	156.101	32.209	29.161	62.499	54.634	35.354	38.867
e.2	154.6316	79.2259	134.4987	26.2074	41.8221	31.2989	37.255	23.887	37.951
e.3	199.1772	202.6345	187.1986	62.7967	62.2389	70.0881	68.959	72.435	71.287
e.4	135.521	133.672	121.839	29.6	39.068	40.448	40.982	34.567	43.538

Table S4. The content of different types of bond orders, water content, and total bond order density.

Lable	PBO (Ca-O)	PBO (Si-O)	PBO (X-O)	PBO (O-H)	PBO (HB)	（H_2O+OH） wt%	TBOD
a.1	18.30%	56.16%	0.00%	22.85%	2.68%	12.32%	0.0246
a.2	18.23%	56.13%	0.00%	22.65%	2.98%	12.32%	0.0244
a.3	22.70%	70.79%	0.00%	6.13%	0.38%	5.16%	0.0234
a.4	14.14%	55.76%	0.00%	27.36%	2.73%	17.91%	0.0252
a.5	15.09%	55.99%	0.00%	28.14%	0.79%	17.91%	0.0242
a.6	16.17%	56.24%	0.00%	25.25%	2.34%	15.04%	0.0242
a.7	16.31%	48.97%	0.00%	31.02%	3.70%	20.40%	0.0226
a.8	22.63%	38.78%	0.00%	33.33%	5.26%	23.15%	0.0230
b.1	29.71%	59.90%	0.00%	10.14%	0.24%	8.05%	0.0219
b.2	10.39%	54.85%	0.00%	32.35%	2.40%	19.26%	0.0256
b.3	26.58%	67.86%	0.00%	5.56%	0.00%	4.76%	0.0224
b.4	43.60%	44.46%	0.00%	11.93%	0.00%	8.13%	0.0192
b.5	23.92%	40.12%	0.00%	28.11%	7.86%	20.46%	0.0247
b.6	33.79%	42.58%	0.00%	21.09%	2.55%	17.88%	0.0213
b.7	40.71%	50.84%	0.00%	8.45%	0.00%	6.36%	0.0210
b.8	40.85%	34.21%	0.00%	24.94%	0.00%	19.98%	0.0190
b.9	24.79%	62.41%	0.00%	10.19%	2.61%	9.28%	0.0241
b.10	19.51%	50.68%	0.00%	23.93%	5.88%	19.39%	0.0254
b.11	30.44%	58.67%	0.00%	9.59%	1.30%	8.05%	0.0224
b.12	43.85%	49.49%	0.00%	6.66%	0.00%	4.46%	0.0197
b.13	43.52%	47.85%	0.00%	8.32%	0.31%	5.76%	0.0194
c.1	28.00%	72.00%	0.00%	0.00%	0.00%	0.00%	0.0223
c.2	36.66%	63.34%	0.00%	0.00%	0.00%	0.00%	0.0207
c.3	19.06%	28.75%	52.19%	0.00%	0.00%	53.95%	0.0268
d.1	31.60%	32.93%	35.48%	0.00%	0.00%	0.00%	0.0226
d.2	30.15%	39.40%	20.55%	9.90%	0.00%	8.37%	0.0227
d.3	24.70%	55.91%	9.76%	9.02%	0.62%	4.33%	0.0231
d.4	39.07%	39.46%	21.47%	0.00%	0.00%	0.00%	0.0219
d.5	40.37%	43.80%	15.84%	0.00%	0.00%	0.00%	0.0220
e.1	18.14%	68.52%	5.85%	5.25%	2.25%	5.12%	0.0249
e.2	18.75%	39.44%	10.85%	26.31%	4.65%	18.80%	0.0256
e.3	34.95%	54.46%	6.88%	3.56%	0.15%	2.33%	0.0188
e.4	38.22%	52.56%	3.69%	5.53%	0.00%	3.64%	0.0194

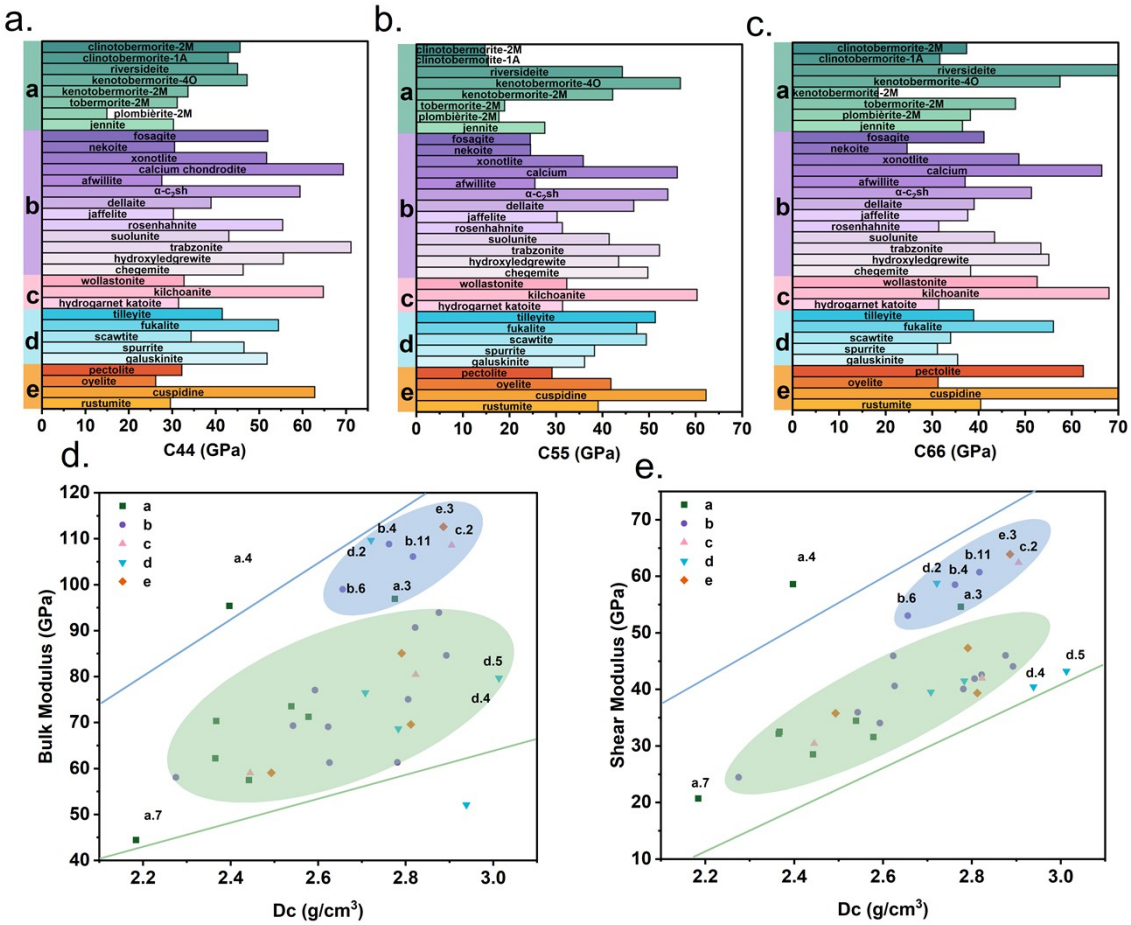

Figure S1. a-c. Distribution of C44, C55, and C66 values in CSH, d-e. Correlation analysis between bulk modulus, shear modulus and density (Dc).

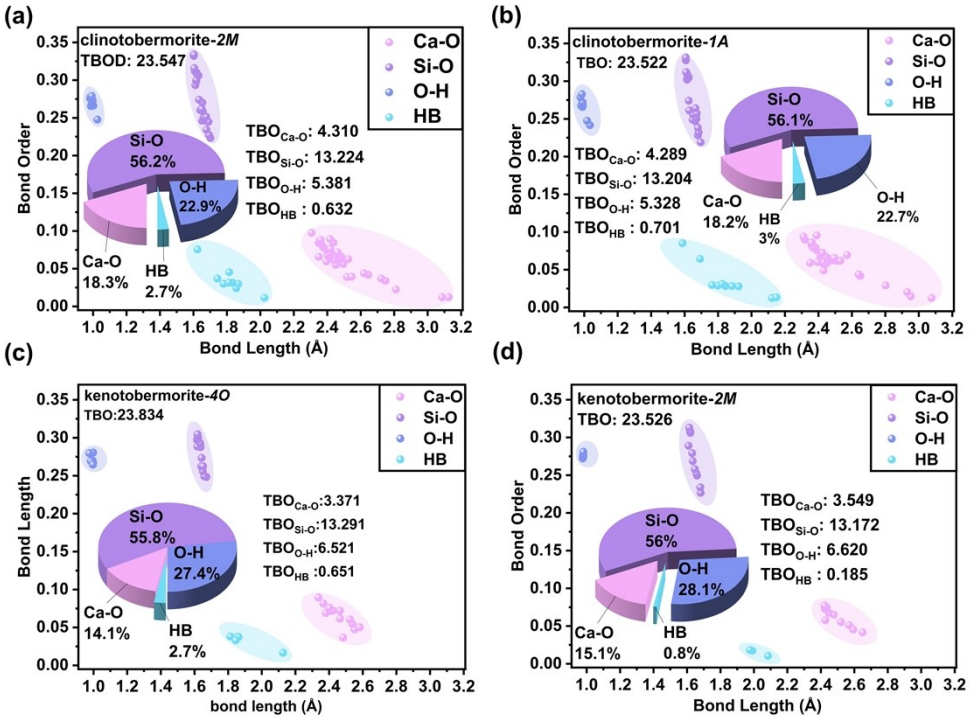

Figure S2. BO of clinotobermorite and kenotobermorite.

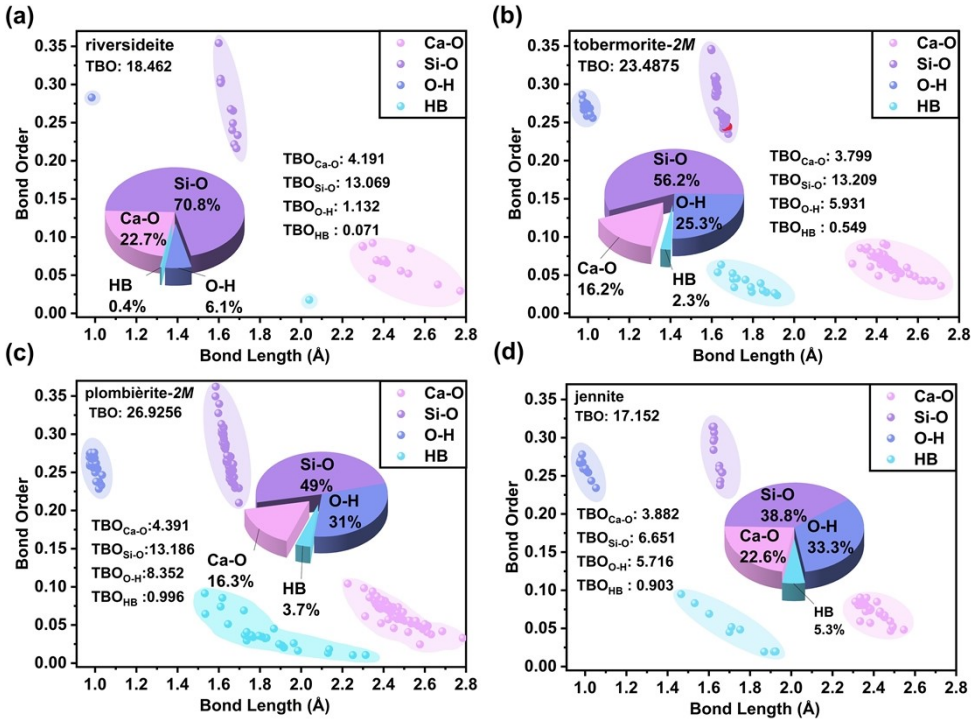

Figure S3. BO of the other tobermorite and jennite.

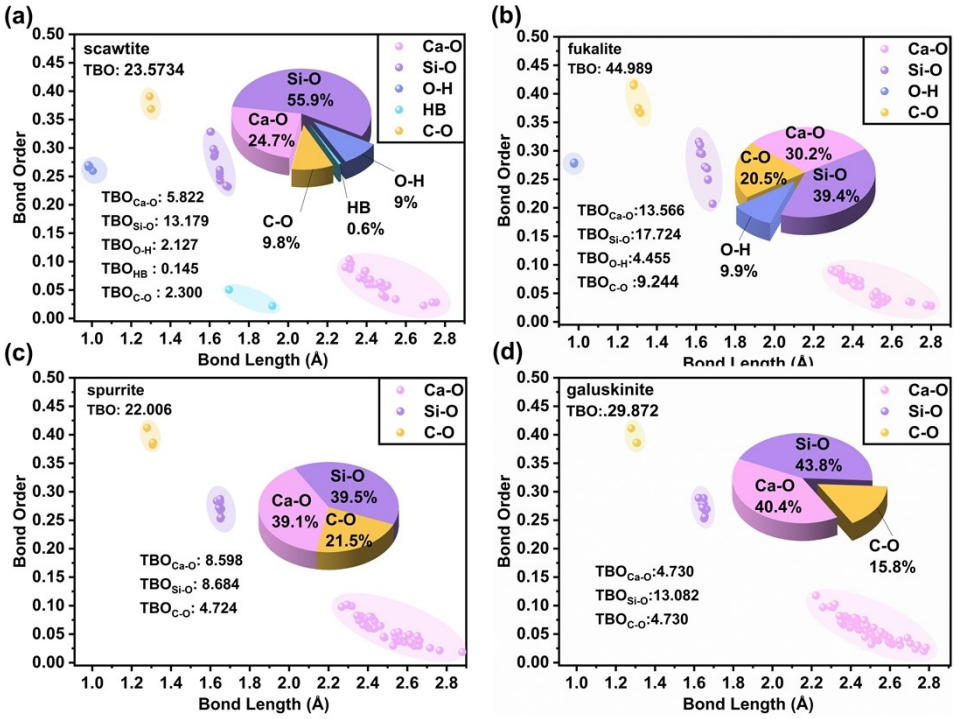

Figure S4. BO-BL of scawtite, fukalite, spurrite, and galuskinite.

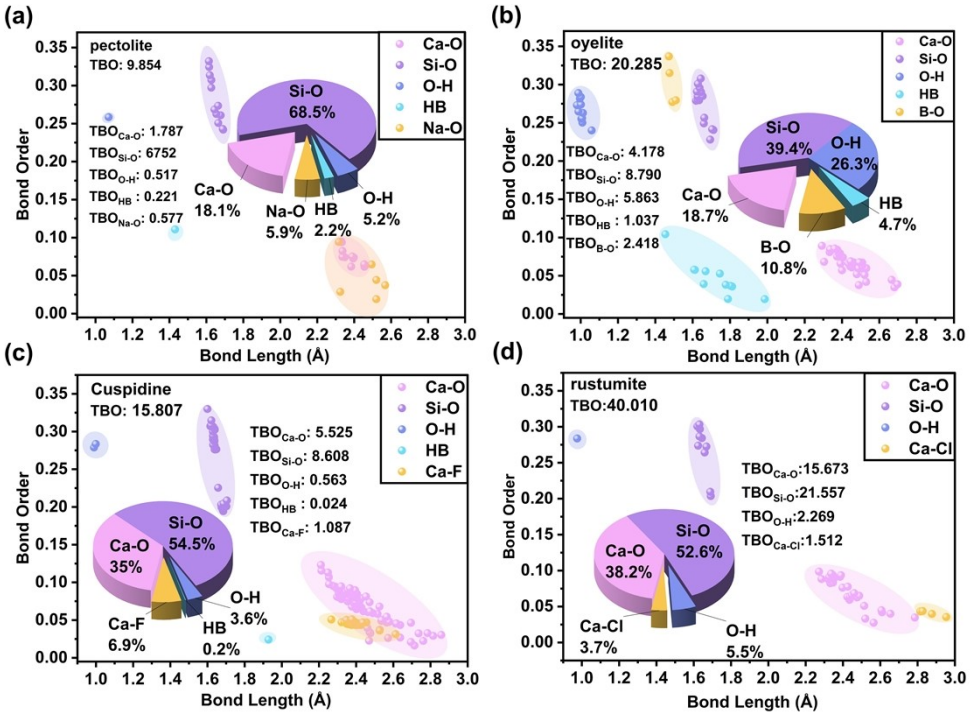

Figure S5. BO-BL distribution for pectolite, oyelite, cuspidine, rustumite.

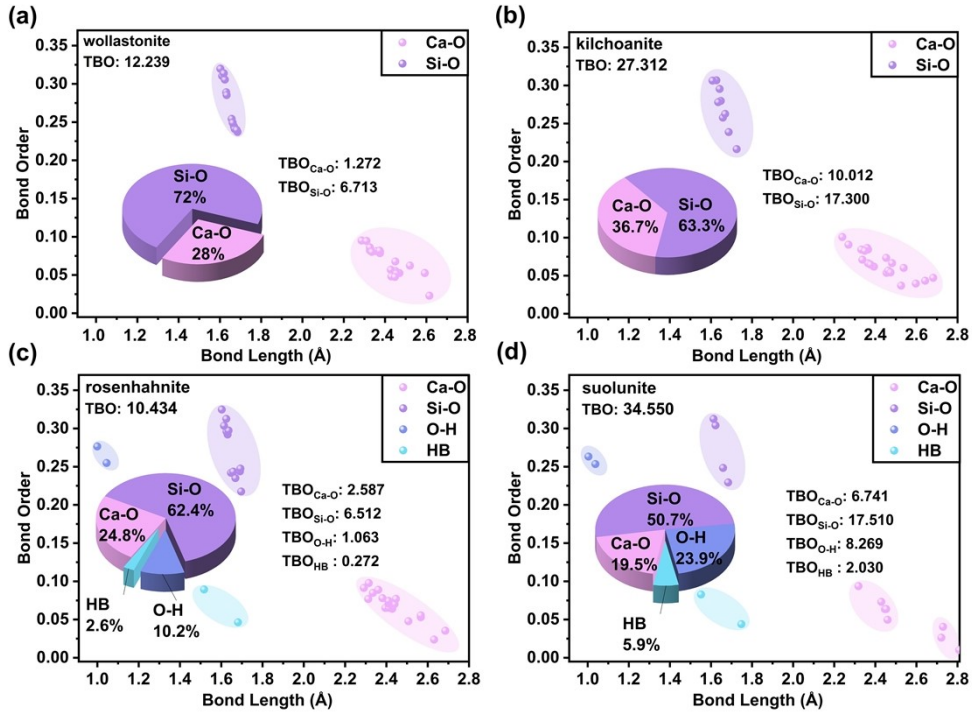

Figure S6. BO-BL distribution for wollastonite, kilchoanite, rosenhahnite and suolunite.

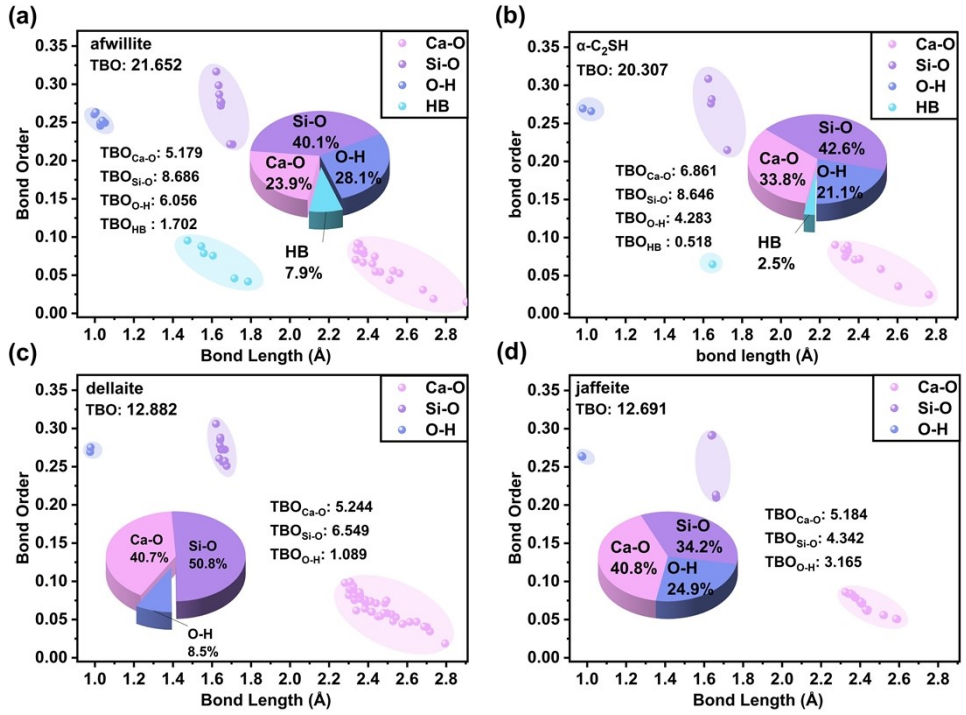

Figure S7 BO-BL distribution for afwillite, α-C_2SH, dellaite and jaffeite.

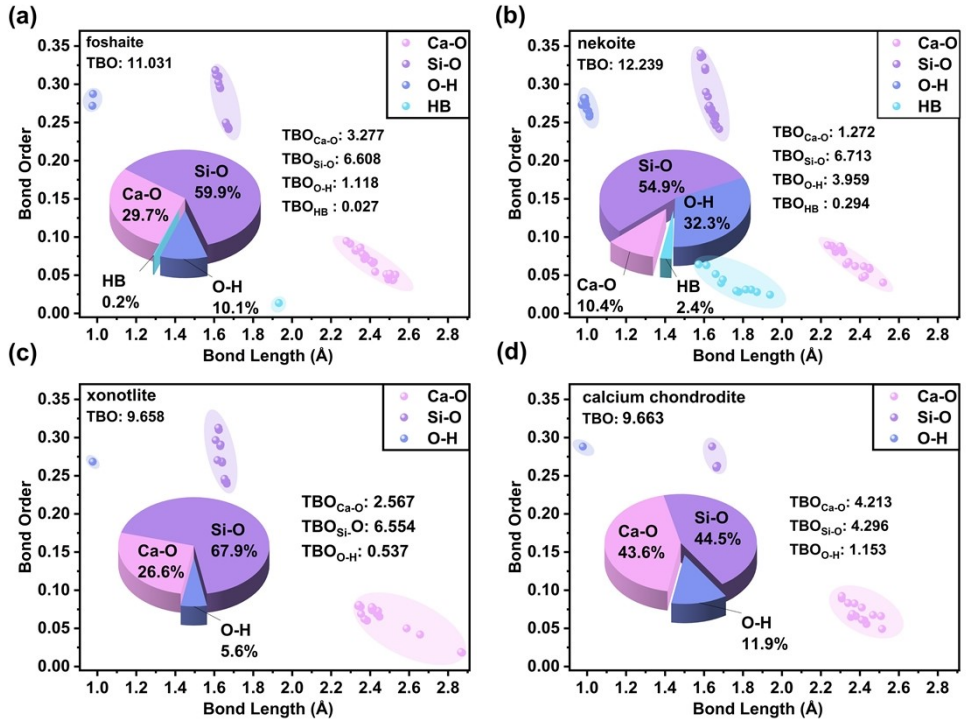

Figure S8. BO-BL distribution for foshagite, nekoite, xonotlite and calcium chondrodite.

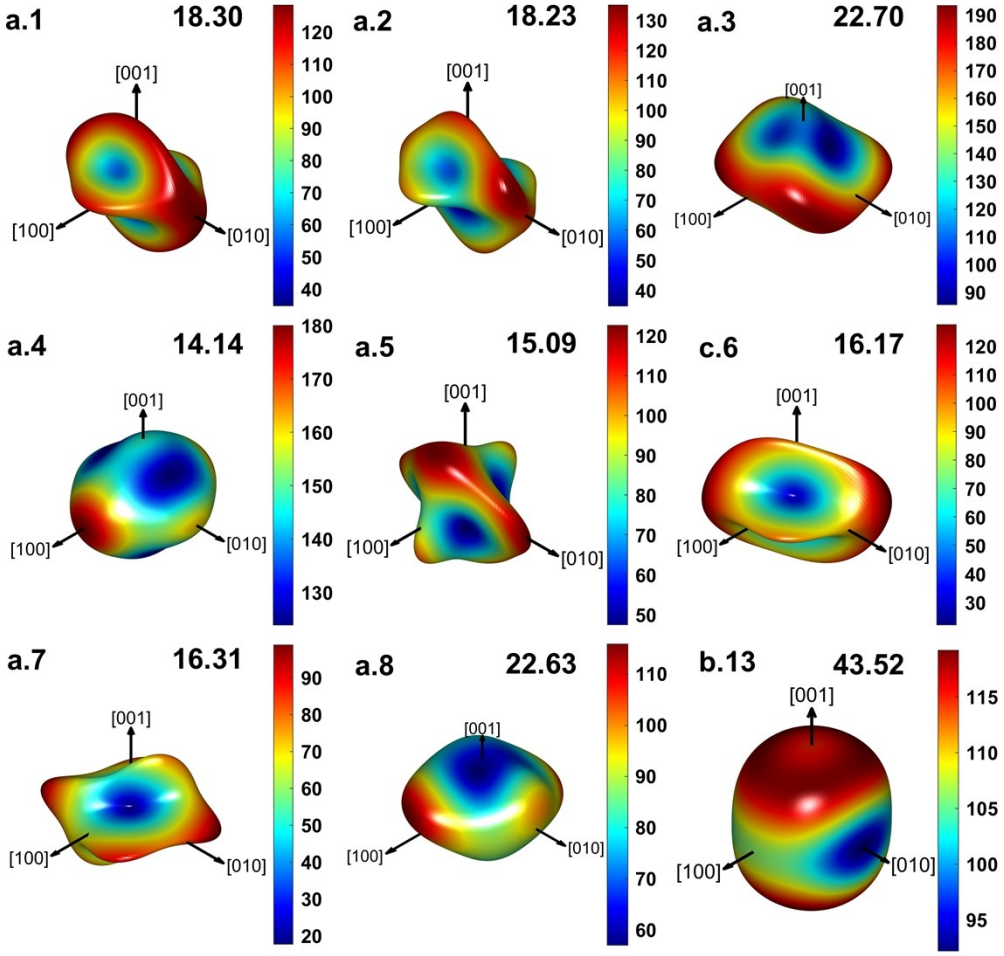

Figure S9. Three-dimensional diagrams of Young's modulus of groups a and b.13.

\

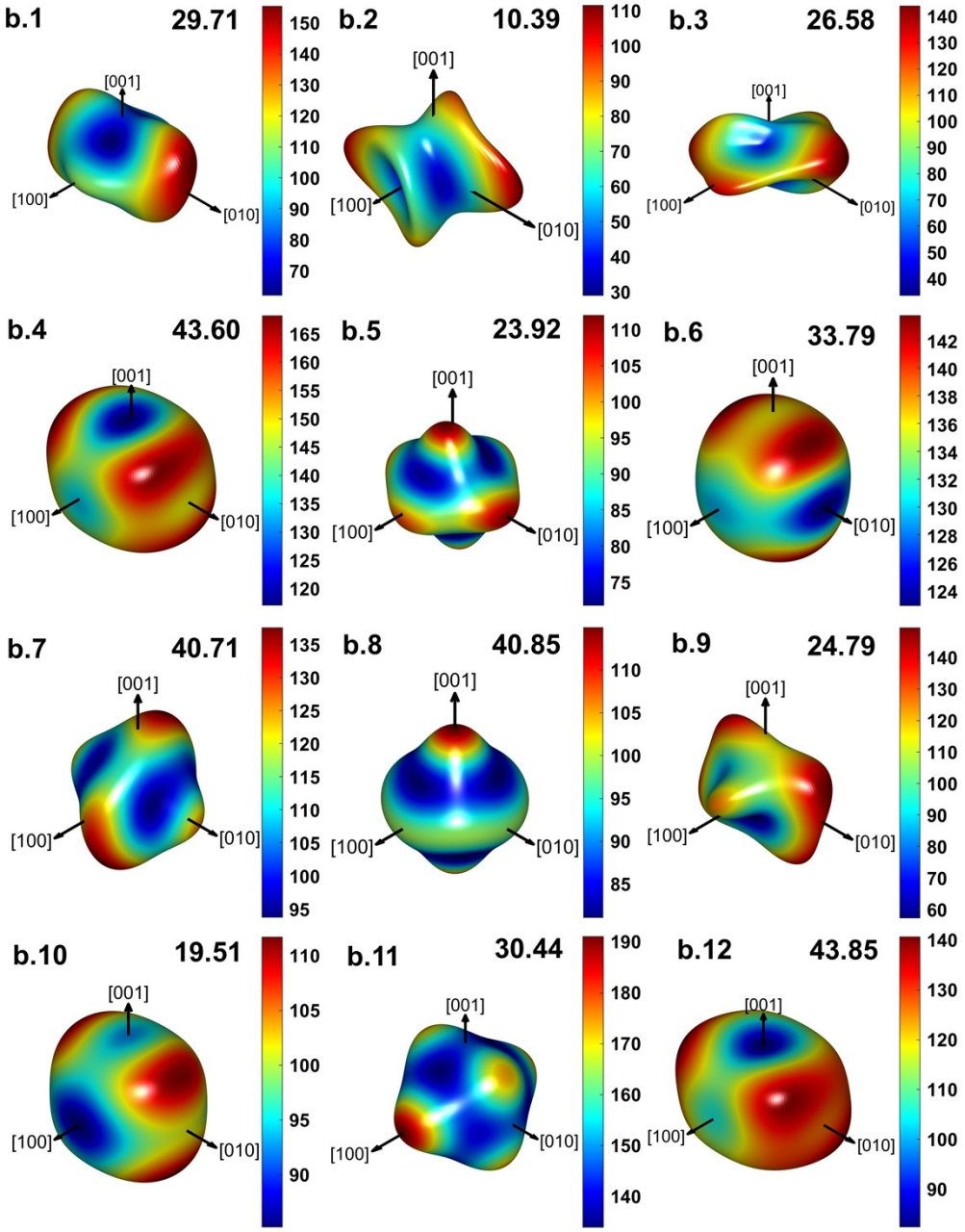

Figure S10. Three-dimensional diagrams of Young's modulus of group b.

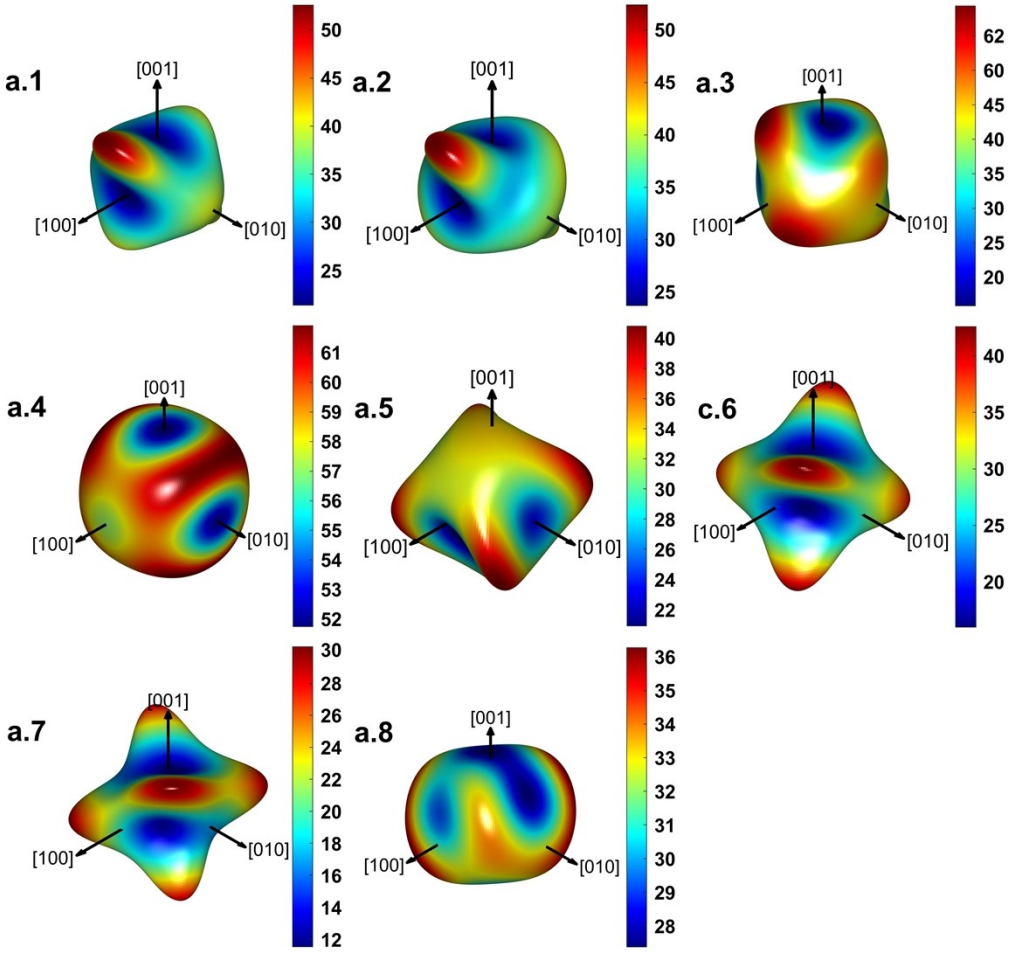

Figure S11. Three-dimensional diagrams of the shear modulus of group a.

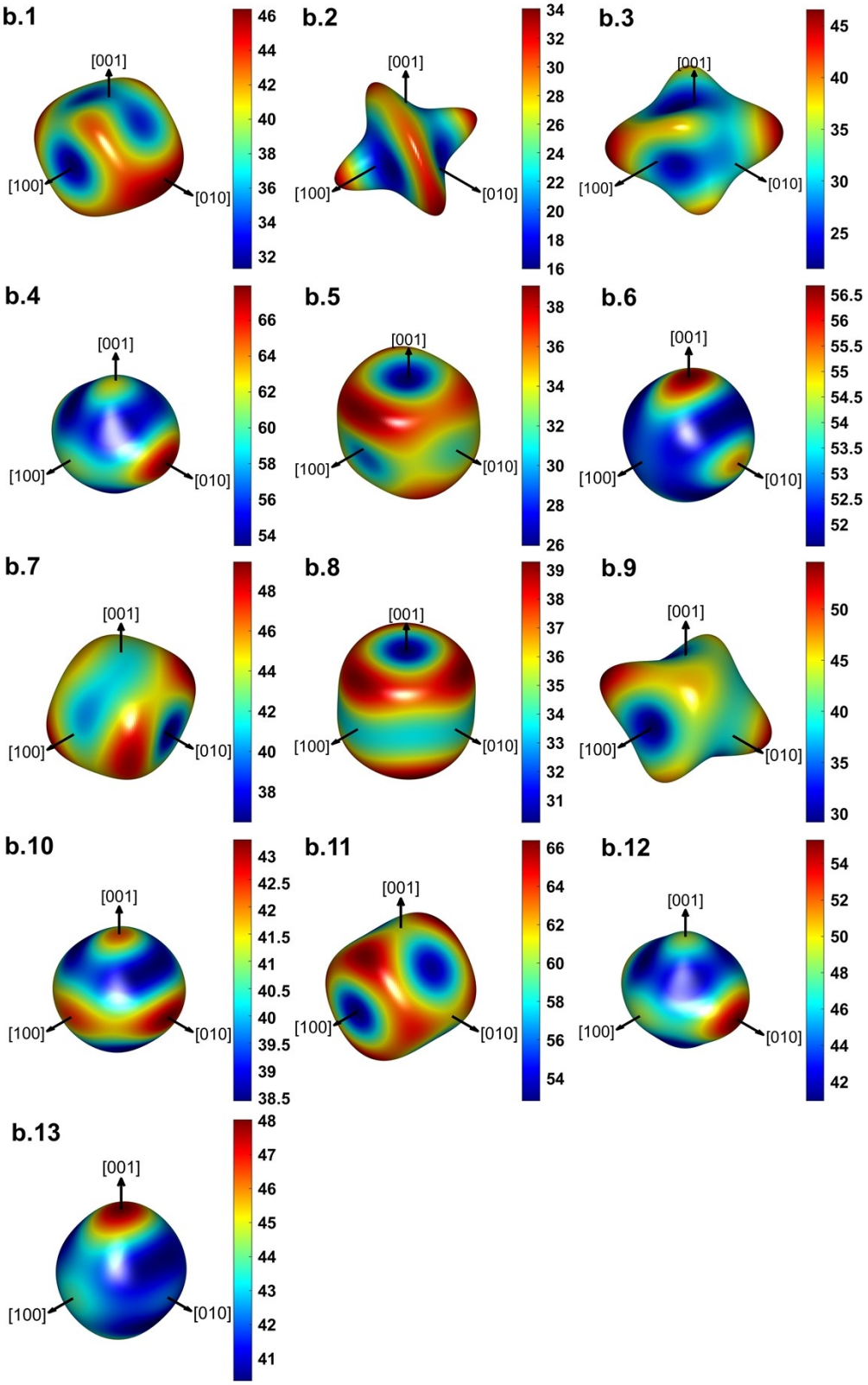

Figure S12. Three-dimensional diagrams of the shear modulus of group b.

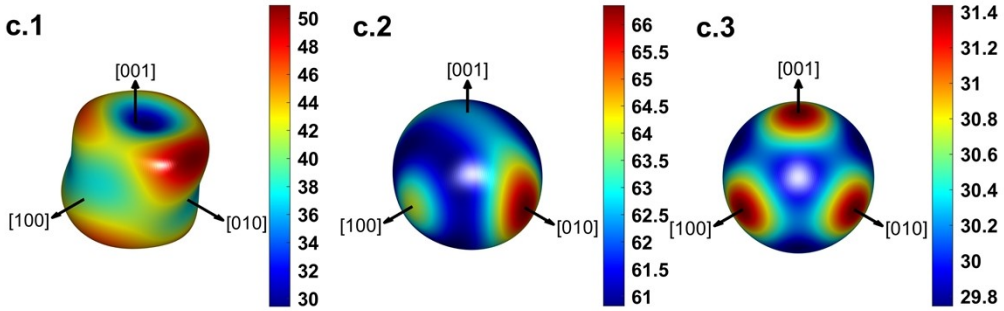

Figure S13. Three-dimensional diagrams of the shear modulus of group c.

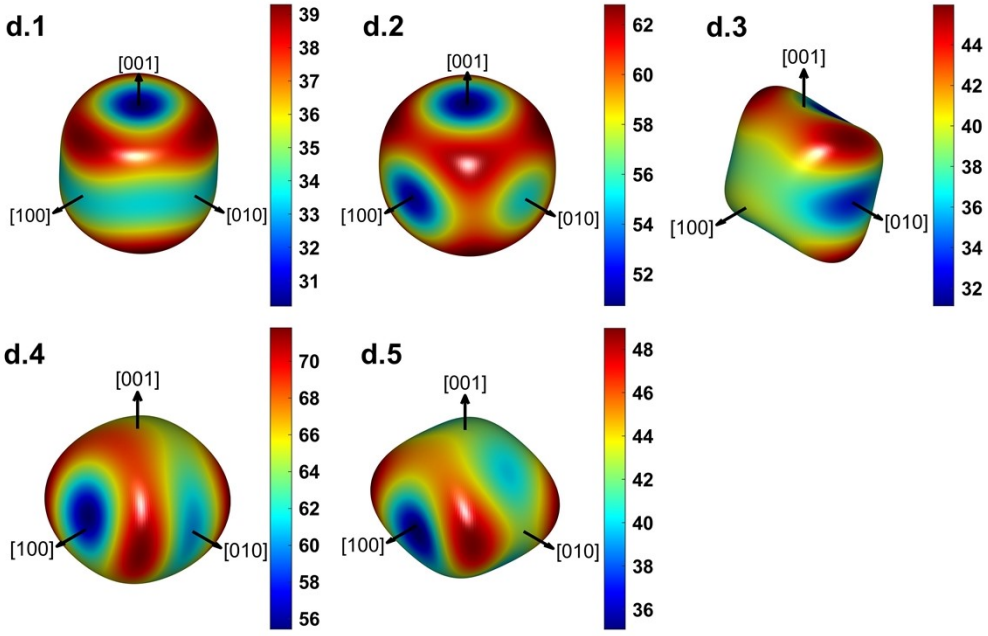

Figure S14. Three-dimensional diagrams of the shear modulus of group d.

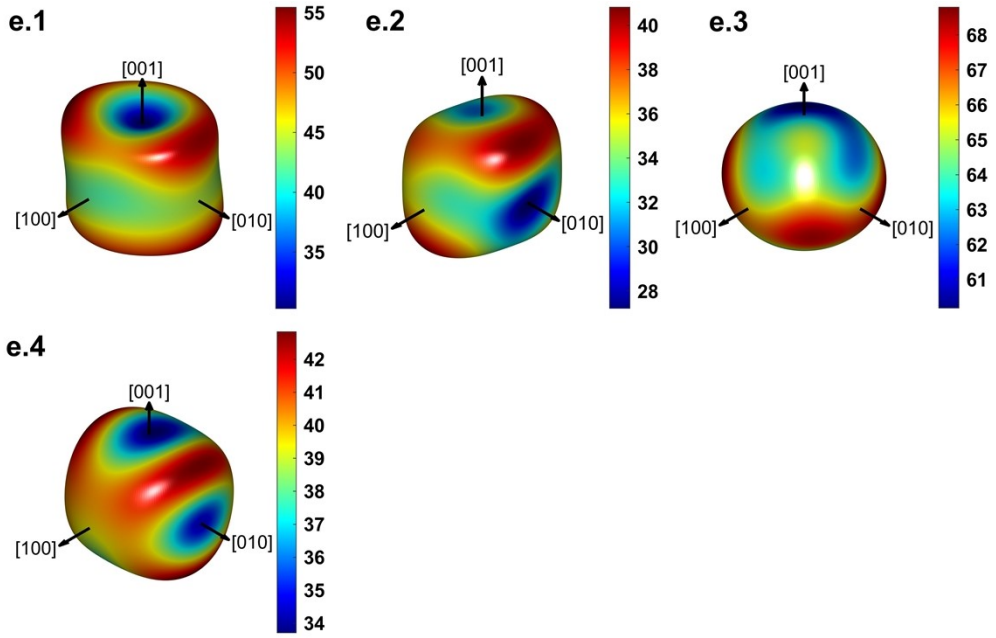

Figure S15. Three-dimensional diagrams of the shear modulus of group e.

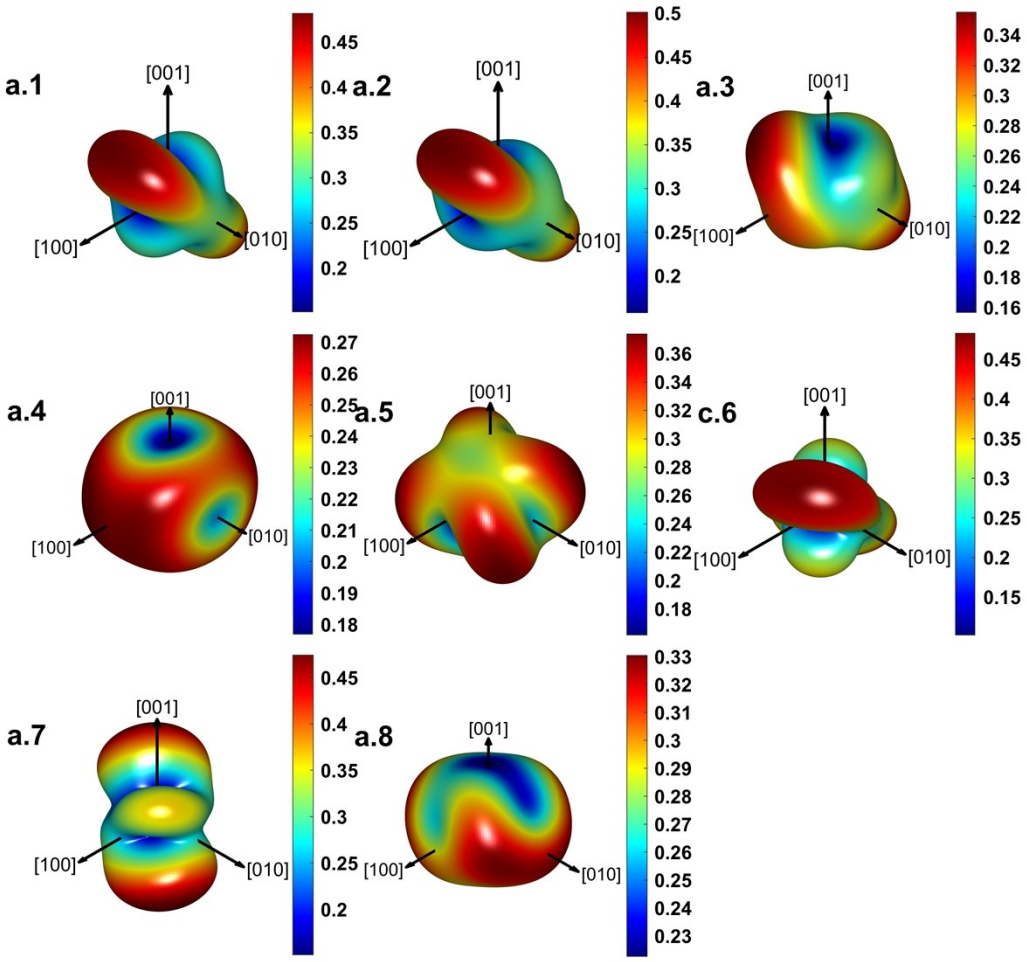

Figure S16. Three-dimensional diagrams of hardness of group a.

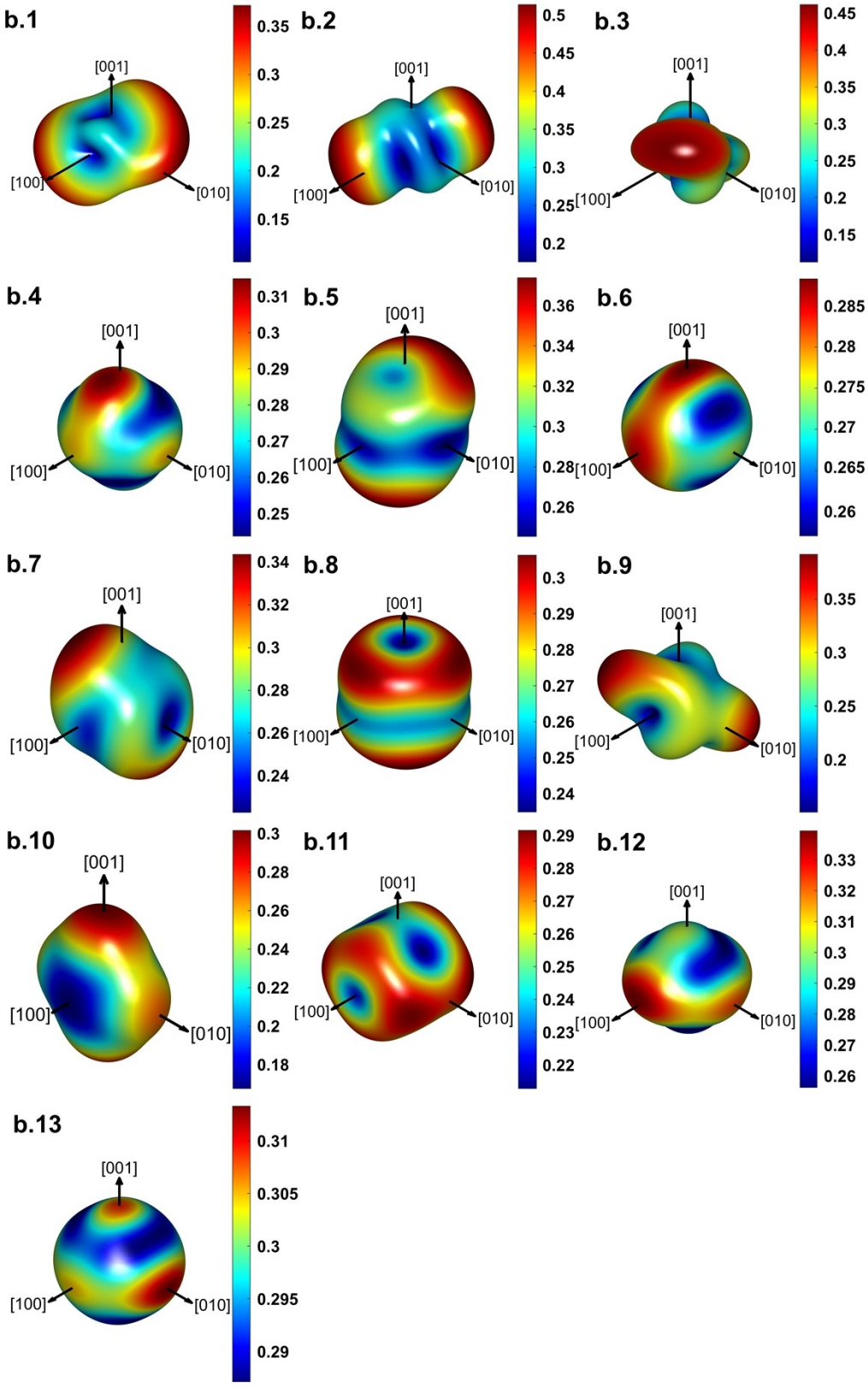

Figure S17. Three-dimensional diagrams of hardness of group b.

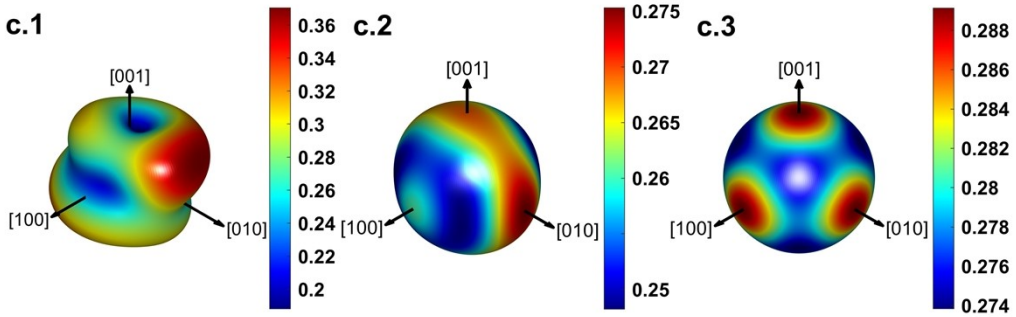

Figure S18. Three-dimensional diagrams of hardness of group c.

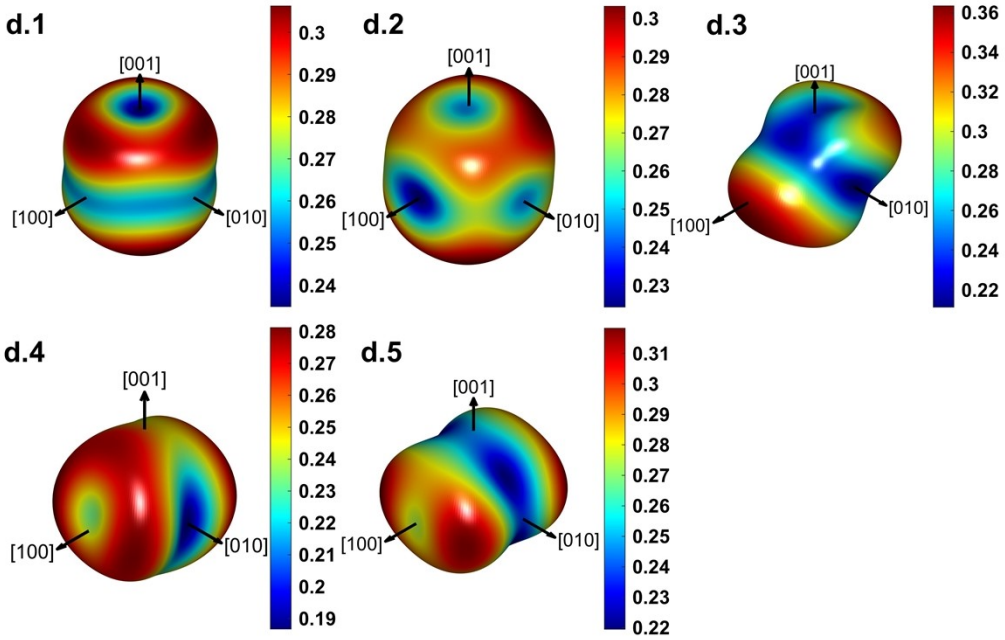

Figure S19. Three-dimensional diagrams of hardness of group d.

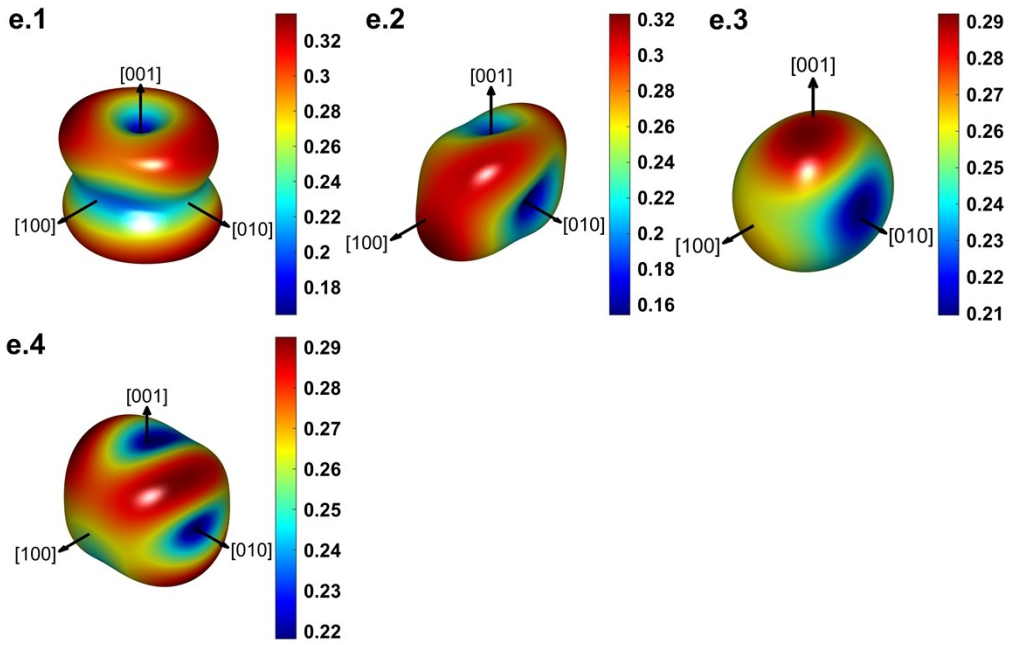

Figure S20. Three-dimensional diagrams of hardness of group e.

References

(1) Nielsen, O. H.; Martin, R. M. First-Principles Calculation of Stress. *Phys. Rev. Lett.* **1983**, *50* (9), 697–700.

(2) Gale, J. D.; Rohl, A. L. The General Utility Lattice Program (GULP). *Molecular Simulation* **2003**, *29* (5), 291–341.

(3) Merlino, S.; Bonaccorsi, E.; Armbruster, T. The Real Structures of Clinotobermorite and Tobermorite 9 Å: OD Character, Polytypes, and Structural Relationships. *ejm* **2000**, *12* (2), 411–429.

(4) Merlino, S.; Bonaccorsi, E.; Armbruster, T. Tobermorites; Their Real Structure and Order-Disorder (OD) Character. *American Mineralogist* **1999**, *84* (10), 1613–1621.

(5) Merlino, S.; Bonaccorsi, E.; Armbruster, T. The Real Structure of Tobermorite 11A: Normal and Anomalous Forms, OD Character and Polytypic Modifications. *ejm* **2001**, *13* (3), 577–590.

(6) Churakov, S. Structural Position of H2O Molecules and Hydrogen Bonding in Anomalous 11 Å Tobermorite. *American Mineralogist* **2009**, *94*, 156–165.

(7) The Crystal Structure of Jennite, $Ca_9Si_6O_{18}(OH)_6 \cdot 8H_2O$. *Cement and Concrete Research* **2004**, *34* (9), 1481–1488.

(8) Gard, J. A.; Taylor, H. F. W. The Crystal Structure of Foshagite. *Acta Cryst* **1960**, *13* (10), 785–793.

(9) Alberti, A.; Galli, E. The Structure of Nekoite, $Ca_3Si_6O_{15} \cdot 7H_2O$, a New Type of Sheet Silicate. *American Mineralogist* **1980**, *65* (11–12), 1270–1276.

(10) Churakov, S. V.; Mandaliev, P. Structure of the Hydrogen Bonds and Silica Defects in the Tetrahedral Double Chain of Xonotlite. *Cement and Concrete Research* **2008**, *38* (3), 300–311.

(11) Kirfel, A.; Hamm, H.-M.; Will, G. The Crystal Structure of Reinhardbraunsite, $Ca_5(SiO_4)_2(OH,F)_2$, a New Mineral of the Calcio-Chondrodite Type. *TMPM Tschermaks Petr. Mitt.* **1983**, *31* (1–2), 137–150.

(12) Malik, K. M. A.; Jeffery, J. W. A Re-Investigation of the Structure of Afwillite. *Acta Cryst B* **1976**, *32* (2), 475–480.

(13) Marsh, R. E. A Revised Structure for α-Dicalcium Silicate Hydrate. *Acta Crystallogr C Cryst Struct Commun* **1994**, *50* (7), 996–997.
(14) Yano, T.; Urabe, K.; Ikawa, H.; Teraushi, T.; Ishizawa, N.; Udagawa, S. Structure of α-Dicalcium Silicate Hydrate. *Acta Crystallogr C Cryst Struct Commun* **1993**, *49* (9), 1555–1559.
(15) Udagawa, S.; Urabe, K.; Natsume, M.; Yano, T. REFINEMENT OF THE CRYSTAL STRUCTURE OF γ-Ca_2SiO_4. No. 2.
(16) Yamnova, N. A.; Sarp, K.; Egorov-Tismenko, Y. K.; Pushcharovski, D. Y.; Dasgupta, G. Crystal Structure of Jaffeite. *Crystallography Reports* **1993**, *38*, 464–467.
(17) Wan, C.; Ghose, S.; Gibbs, G. V. Rosenhahnite, $Si_3O_8(OH)_2$; Crystal Structure and the Stereochemical Configuration of the Hydroxylated Trisilicate Group, [$Si_3O_8(OH)_2$]. *American Mineralogist* **1977**, *62* (5–6), 503–512.
(18) Ma, Z.; Shi, N.; Mou, G.; Liao, L. Crystal Structure Refinement of Suolunite and Its Significance to the Cement Techniques. *Chin. Sci. Bull.* **1999**, *44* (23), 2125–2130.
(19) Armbruster, T.; Lazic, B.; Galuskina, I. O.; Galuskin, E. V.; Gnos, E.; Marzec, K. M.; Gazeev, V. M. Trabzonite, $Ca_4[Si_3O_9(OH)]OH$: Crystal Structure, Revised Formula, New Occurrence and Relation to Killalaite. *Mineralogical Magazine* **2012**, *76* (3), 455–472.
(20) Galuskin, E. V.; Lazic, B.; Armbruster, T.; Galuskina, I. O.; Pertsev, N. N.; Gazeev, V. M.; Włodyka, R.; Dulski, M.; Dzierżanowski, P.; Zadov, A. E.; Dubrovinsky, L. S. Edgrewite $Ca_9(SiO_4)_4F_2$-Hydroxyledgrewite $Ca_9(SiO_4)_4(OH)_2$, a New Series of Calcium Humite-Group Minerals from Altered Xenoliths in the Ignimbrite of Upper Chegem Caldera, Northern Caucasus, Kabardino-Balkaria, Russia. *American Mineralogist* **2012**, *97* (11–12), 1998–2006.
(21) Galuskin, E. V.; Gazeev, V. M.; Lazic, B.; Armbruster, T.; Galuskina, I. O.; Zadov, A. E.; Pertsev, N. N.; Wrzalik, R.; Dzierżanowski, P.; Gurbanov, A. G.; Bzowska, G. Chegemite $Ca_7(SiO_4)_3(OH)_2$ a New Humite-Group Calcium Mineral from the Northern Caucasus, Kabardino-Balkaria, Russia. *European Journal of Mineralogy* **2009**, 1045–1059.
(22) Ohashi, Y. Polysynthetically-Twinned Structures of Enstatite and Wollastonite. *Phys Chem Minerals* **1984**, *10* (5), 217–229.
(23) Taylor, H. F. W. The Crystal Structure of Kilchoanite, $Ca_6(SiO_4)(Si_3O_{10})$, with Some Comments on Related Phases. *Mineralogical Magazine* **1971**, *38* (293), 26–31.
(24) Cohen-Addad, M.; Ducros, P.; Durif-Varambon, A.; Bertaut, E. F.; Delapalme, A. Etude de La Position Des Atomes d'hydrogene Dans l'hydrogrenat Al_2O_3,3CaO,6H_2O. *Solid State Communications* **1963**, *1* (4), 85–87.
(25) Lottisnatham, S. J.; Smith, J. V. Crystal Structure of Tilleyite: Refinement and Coordination. *Zeitschrift für Kristallographie - Crystalline Materials* **1970**, *132*, 288–306.
(26) Rastsvetaeva, R.; Bolotina, N.; Zadov, A. E.; Chukanov, N. Crystal Structure of Fukalite Dimorph ($Ca_4[Si_2O_6](CO_3)$ $(OH)_2$ from the Gumeshevsk Deposit, the Urals. *Doklady Earth Sciences* **2005**, *405*, 1347–1351.
(27) Pluth, J. J.; Smith, J. V. The Crystal Structure of Scawtite, $Ca_7(Si_6O_{18})(CO_3)\cdot 2H_2O$. *Acta Crystallographica Section B* **1973**, *29* (1), 73–80.
(28) Smith, J. V.; Karle, I. L.; Hauptman, H.; Karle, J. The Crystal Structure of Spurrite, $Ca_5(SiO_4)_2CO_3$. II. Description of Structures. *Acta Crystallographica* **1960**, *13* (6), 454–458.
(29) Lazic, B.; Armbruster, T.; Savelyeva, V. B.; Zadov, A. E.; Pertsev, N. N.; Dzierżanowski, P. Galuskinite, $Ca_7(SiO_4)_3(CO_3)$, a New Skarn Mineral from the Birkhin Gabbro Massif, Eastern Siberia, Russia. *Mineral. mag.* **2011**, *75* (5), 2631–2648.

(30) Hydrogen Bonding and Cation Ordering in Magnet Cove Pectolite. *Zeitschrift für Kristallographie - Crystalline Materials* **1977**, *146* (4–6), 281–292.
(31) Pekov, I. V.; Zubkova, N. V.; Chukanov, N. V.; Yapaskurt, V. O.; Britvin, S. N.; Kasatkin, A. V.; Pushcharovsky, D. Y. Oyelite: New Mineralogical Data, Crystal Structure Model and Refined Formula $Ca_5BSi_4O_{13}(OH)_3 \cdot 4H_2O$. *ejm* **2019**, *31* (3), 595–608.
(32) Saburi, S.; Kawahara, A.; Henmi, C.; Kusachi, I.; Kihara, K. The Refinement of the Crystal Structure of Cuspidine. *Mineralogical Journal* **1977**, *8* (5), 286–298.
(33) HOWIE, R. A.; ILYUKHIN, V. V. Crystal Structure of Rustumite. *Nature* **1977**, *269* (5625), 231–231.